




# Archetypal Analysis++: Rethinking the Initialization Strategy

Sebastian Mair <sup>1</sup>  and Jens Sjölund <sup>1</sup>

<sup>1</sup>Uppsala University, Sweden

---

## Abstract

Archetypal analysis is a matrix factorization method with convexity constraints. Due to local minima, a good initialization is essential. Frequently used initialization methods yield either sub-optimal starting points or are prone to get stuck in poor local minima. In this paper, we propose archetypal analysis++ (AA++), a probabilistic initialization strategy for archetypal analysis that sequentially samples points based on their influence on the objective, similar to  $k$ -means++. In fact, we argue that  $k$ -means++ already approximates the proposed initialization method. Furthermore, we suggest to adapt an efficient Monte Carlo approximation of  $k$ -means++ to AA++. In an extensive empirical evaluation of 13 real-world data sets of varying sizes and dimensionalities and considering two pre-processing strategies, we show that AA++ almost consistently outperforms all baselines, including the most frequently used ones.

---

## 1 Introduction

Archetypal analysis (AA) (Cutler and Breiman, 1994) is a matrix factorization method with convexity constraints. The idea is to represent every data point as a convex combination of points, called archetypes, located on the boundary of the data set. Thus, archetypes can be seen as well-separated observations that summarize the most relevant extremes of the data. The convexity constraints also give archetypal analysis a natural interpretation.

Archetypal analysis has been applied, e.g., for global gene expression (Thøgersen et al., 2013), bioinformatics (Hart et al., 2015), apparel design (Vinué et al., 2015), chemical spaces of small organic molecules (Keller et al., 2021), geophysical data (Black et al., 2022), large-scale climate drivers (Hannachi and Trendafilov, 2017; Chapman et al., 2022), and population genetics (Gimbernat-Mayol et al., 2022).

To improve the computation of archetypal analysis, various optimization approaches (Bauckhage and Thureau, 2009; Mørup and Hansen, 2012; Chen et al., 2014; Bauckhage et al., 2015; Abrol and Sharma, 2020) and approximations (Mair et al., 2017; Damle and Sun, 2017; Mei et al., 2018; Mair and Brefeld, 2019; Han et al., 2022) have been proposed. However, the earliest point of attack for obtaining a good solution is the initialization of the archetypes. Surprisingly, this has barely been investigated.

In the original paper, Cutler and Breiman (1994) use a random initialization, i.e., choosing random points from the data set, which was adopted by many others, e.g., (Eugster and Leisch, 2011; Seth and Eugster, 2015; Hinrich et al., 2016; Hannachi and Trendafilov, 2017; Mair et al., 2017; Mei et al., 2018; Krohne et al., 2019; Olsen et al., 2022) to name a few. Furthermore, Cutler and Breiman (1994) state that a careful initialization improves the convergence speed and that archetypes should not be initialized too close to each other.

The same idea serves as an argument for using the *FurthestFirst* approach (Gonzalez, 1985; Hochbaum and Shmoys, 1985), yielding a well-separated initialization used, e.g., in  $k$ -means clustering (Lloyd, 1982). Inspired by *FurthestFirst*, Mørup and Hansen (2010, 2012) propose a modification for archetypal analysis called *FurthestSum*, which focuses on boundary points rather than well-separated points. Here, boundary points refer to points on the boundary of the convex hull of the data. Since then, *FurthestSum* has established itself as one of the default initialization strategies for archetypal analysis (Thøgersen et al., 2013; Hinrich et al., 2016; Mair and Brefeld, 2019; Abrol and Sharma, 2020; Beck et al., 2022; Black et al., 2022; Chapman et al., 2022; Gimbernat-Mayol et al., 2022).

 **For correspondence:**  
sebastian.mair@it.uu.se

**Funding:** This work was partially supported by the Wallenberg AI, Autonomous Systems and Software Program (WASP) funded by the Knut and Alice Wallenberg Foundation.

**Code:** The code is available on request and will be published on github once the paper is peer-reviewed.

arXiv:2301.13748v1 [cs.LG] 31 Jan 2023

Despite its popularity, FurthestSum has also been criticized. For example, Suleman (2017) states that FurthestSum is prone to selecting redundant archetypes, primarily when many archetypes are used. Redundant archetypes lie in the convex hull of the already selected archetypes and thus do not lower the overall error. In addition, Krohne et al. (2019) and Olsen et al. (2022) report better results with a random initialization than with FurthestSum. A possible explanation is that FurthestSum’s early focus on boundary points risks trapping it in poor local minima.

## Contributions

In this paper, we motivate and propose archetypal analysis++ (AA++), an initialization strategy inspired by  $k$ -means++ (Arthur and Vassilvitskii, 2007; Ostrovsky et al., 2013). Furthermore, we argue that the  $k$ -means++ initialization can be seen as an approximation to the proposed AA++ strategy and that a Monte Carlo approximation to the  $k$ -means++ initialization can be adapted for AA++ for a more efficient initialization. Most importantly, we empirically demonstrate that our proposed AA++ initialization for archetypal analysis outperforms almost consistently all baselines on 13 real-world data sets.

## 2 Preliminaries

Before introducing archetypal analysis, we briefly revisit  $k$ -means clustering since we will build upon similar ideas.

### 2.1 $k$ -means Clustering

Let  $\mathcal{X} \subset \mathbb{R}^d$  be a data set of  $n$  points in  $d$  dimensions and let  $\mathcal{Z} = \{\mathbf{z}_1, \dots, \mathbf{z}_k\}$  be a set of  $k$  cluster centers. Consider the  $k$ -means clustering problem with the following objective

$$\phi_{\mathcal{X}}(\mathcal{Z}) = \sum_{\mathbf{x} \in \mathcal{X}} d(\mathbf{x}, \mathcal{Z})^2 = \sum_{\mathbf{x} \in \mathcal{X}} \min_{\mathbf{q} \in \{\mathbf{z}_1, \dots, \mathbf{z}_k\}} \|\mathbf{x} - \mathbf{q}\|_2^2,$$

where  $d(\mathbf{x}, \mathcal{Z})^2 = \min_{\mathbf{q} \in \mathcal{Z}} \|\mathbf{x} - \mathbf{q}\|_2^2$  is the minimal squared distance from a data point  $\mathbf{x}$  to the closest center in  $\mathcal{Z}$ .

Often, the cluster centers  $\mathcal{Z}$  of  $k$ -means are initialized using the  $k$ -means++ initialization procedure (Arthur and Vassilvitskii, 2007), which works as follows. The first center is chosen uniformly at random. Then, the remaining  $k - 1$  cluster centers are chosen according to a probability distribution where the probability of choosing a point  $\mathbf{x}$  is proportional to the closest distance to the already chosen cluster centers, i.e.,  $p(\mathbf{x}) \propto d(\mathbf{x}, \mathcal{Z})^2$ . The procedure is outlined in Algorithm 1.

### 2.2 Archetypal Analysis

Let  $\mathcal{X} = \{\mathbf{x}_1, \dots, \mathbf{x}_n\}_{i=1}^n \subset \mathbb{R}^d$  be a data set consisting of  $n \in \mathbb{N}$   $d$ -dimensional data points arranged as rows in the design matrix  $\mathbf{X} \in \mathbb{R}^{n \times d}$ . The idea in archetypal analysis (AA) (Cutler and Breiman, 1994) is to (approximately) represent every data point  $\mathbf{x}_i$  as a convex combination of  $k \in \mathbb{N}$  archetypes  $\mathcal{Z} = \{\mathbf{z}_1, \dots, \mathbf{z}_k\}$ , i.e.,

$$\mathbf{x}_i^\top \approx \mathbf{a}_i^\top \mathbf{Z}, \quad \mathbf{a}_i^\top \mathbf{1} = 1, \quad \mathbf{a}_i \geq 0,$$

---

#### Algorithm 1 $k$ -means++ Initialization

---

- 1: **Input:** Set of  $n$  data points  $\mathcal{X}$ , number of clusters  $k$
  - 2: **Output:** Initial set of clusters centers  $\mathcal{Z}$
  - 3: Sample index  $i$  uniformly at random from  $[n]$ , i.e.,  
using  $p(i) = n^{-1}$
  - 4: Append  $\mathbf{x}_i$  to  $\mathcal{Z}$
  - 5: **while**  $|\mathcal{C}| < k$  **do**
  - 6:   Sample  $i$  using  $p(i) \propto \min_{\mathbf{z} \in \mathcal{Z}} \|\mathbf{x}_i - \mathbf{z}\|_2^2$
  - 7:   Append  $\mathbf{x}_i$  to  $\mathcal{Z}$
  - 8: **end while**
-

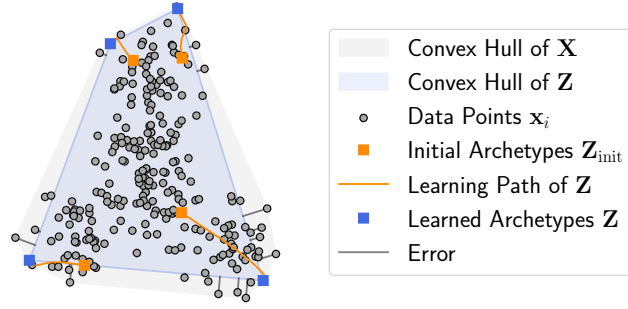


**Figure 1.** Archetypal analysis in two dimensions with  $k = 4$ .

where the matrix  $\mathbf{Z} \in \mathbb{R}^{k \times d}$  contains the archetypes as rows and the vector  $\mathbf{a}_i \in \mathbb{R}^k$  defines the weights for the  $i$ th data point. Besides,  $\mathbf{1}$  denotes the vector of ones and  $\mathbf{a}_i \geq 0$  is meant element-wise. The archetypes  $\mathbf{z}_j$  ( $j = 1, \dots, k$ ) themselves are also represented (exactly) as convex combinations, but of the data points, i.e.,

$$\mathbf{z}_j^\top = \mathbf{b}_j^\top \mathbf{X}, \quad \mathbf{b}_j^\top \mathbf{1} = 1, \quad \mathbf{b}_j \geq 0,$$

where  $\mathbf{b}_j \in \mathbb{R}^n$  is the weight vector of the  $j$ th archetype. Let  $\mathbf{A} \in \mathbb{R}^{n \times k}$  and  $\mathbf{B} \in \mathbb{R}^{k \times n}$  be the matrices consisting of the weights  $\mathbf{a}_i$  ( $i = 1, \dots, n$ ) and  $\mathbf{b}_j$  ( $j = 1, \dots, k$ ). Then, archetypal analysis yields an approximate factorization of the design matrix as follows

$$\mathbf{X} \approx \mathbf{A}\mathbf{B}\mathbf{X} = \mathbf{A}\mathbf{Z}, \quad (1)$$

where  $\mathbf{Z} = \mathbf{B}\mathbf{X} \in \mathbb{R}^{k \times d}$  is the matrix of archetypes. Due to the convexity constraints, the weight matrices  $\mathbf{A}$  and  $\mathbf{B}$  are row-stochastic. The weight matrices  $\mathbf{A}$  and  $\mathbf{B}$  are typically determined by minimizing the approximation error in the Frobenius norm, resulting in the optimization problem

$$\begin{aligned} & \underset{\mathbf{A}, \mathbf{B}}{\text{minimize}} && \|\mathbf{X} - \mathbf{A}\mathbf{B}\mathbf{X}\|_F^2 \\ & \text{subject to} && \mathbf{A}\mathbf{1} = \mathbf{1}, \mathbf{A} \geq 0, \mathbf{B}\mathbf{1} = \mathbf{1}, \mathbf{B} \geq 0. \end{aligned} \quad (2)$$

This can be equivalently expressed as minimizing the sum of projections of the data points on the archetype-induced convex hull as follows

$$\|\mathbf{X} - \mathbf{A}\mathbf{Z}\|_F^2 = \sum_{\mathbf{x} \in \mathcal{X}} \min_{\mathbf{q} \in \text{conv}(\{\mathbf{z}_1, \dots, \mathbf{z}_k\})} \|\mathbf{x} - \mathbf{q}\|_2^2, \quad (3)$$

where  $\text{conv}(S)$  refers to the convex hull of a set  $S$ . An example of archetypal analysis and projection errors is depicted in Figure 1. The optimization problem is a generalized low-rank problem (Udell et al., 2016), which is biconvex but not convex. Because it is biconvex, a local optimum can be found via an alternating optimization scheme such as the standard one outlined in Algorithm 2. However, the quality of this local optimum is directly dependent on the initialization.

### 2.3 Archetype Initializations

Popular ways of initializing the archetypes  $\mathbf{Z}$  is by using uniformly at random chosen data points or the FurthestSum procedure (Mørup and Hansen, 2010, 2012), but we also introduce FurthestFirst.

#### FurthestFirst

Originally proposed for the metric  $k$ -center problem, the *FurthestFirst* algorithm (Gonzalez, 1985; Hochbaum and Shmoys, 1985) selects the first center/archetype at random and selects every consecutive point which is furthest away from the closest already selected center/archetype. Mathematically, the index of the next point is

$$j^{\text{next}} = \arg \max_{i \in [n]} \left( \min_{\mathbf{q} \in \mathcal{Z}} \|\mathbf{x}_i - \mathbf{q}\|_2^\alpha \right),$$

where  $[n] = \{1, 2, \dots, n\}$  and  $\alpha = 1$ . Note that in  $k$ -means++, the distances are squared, i.e.,  $\alpha = 2$ , and that points are sampled.

---

**Algorithm 2** Archetypal Analysis (Cutler and Breiman, 1994)

---

- 1: **Input:** data matrix  $\mathbf{X}$ , number of archetypes  $k$
  - 2: **Output:** weight matrices  $\mathbf{A}$  and  $\mathbf{B}$
  - 3:  $\mathbf{Z} \leftarrow$  initialization of the archetypes  $\mathbf{Z}$
  - 4: **while** not converged **do**
  - 5:    $\mathbf{a}_i = \arg \min_{\mathbf{a}_i^\top \mathbf{1}=1, \mathbf{a}_i \geq 0} \|\mathbf{Z}^\top \mathbf{a}_i - \mathbf{x}_i\|_2^2 \quad \forall i = 1, \dots, n$
  - 6:    $\mathbf{Z} = (\mathbf{A}^\top \mathbf{A})^{-1} \mathbf{A}^\top \mathbf{X}$
  - 7:    $\mathbf{b}_j = \arg \min_{\mathbf{b}_j^\top \mathbf{1}=1, \mathbf{b}_j \geq 0} \|\mathbf{X}^\top \mathbf{b}_j - \mathbf{z}_j\|_2^2 \quad \forall j = 1, \dots, k$
  - 8:    $\mathbf{Z} = \mathbf{B}\mathbf{X}$
  - 9: **end while**
- 

---

**Algorithm 3** Archetypal Analysis++ Initialization

---

- 1: **Input:** Set of  $n$  data points  $\mathcal{X}$ , number of archetypes  $k$
  - 2: **Output:** Initial set of archetypes  $\mathcal{Z}$
  - 3: Sample index  $i$  uniformly at random from  $[n]$ , i.e., using  $p(i) = n^{-1}$
  - 4: Append  $\mathbf{x}_i$  to  $\mathcal{Z}$
  - 5: **while**  $|\mathcal{Z}| < k$  **do**
  - 6:   Sample  $i$  using  $p(i) \propto \min_{\mathbf{q} \in \text{conv}(\mathcal{Z})} \|\mathbf{x}_i - \mathbf{q}\|_2^2$
  - 7:   Append  $\mathbf{x}_i$  to  $\mathcal{Z}$
  - 8: **end while**
- 

### FurthestSum

Specifically for archetypal analysis, Mørup and Hansen (2010, 2012) propose a modification of FurthestFirst called *FurthestSum*, which sums over the distances of the already selected points, i.e.,

$$j^{\text{next}} = \arg \max_{i \in [n]} \left( \sum_{\mathbf{q} \in \mathcal{Z}} \|\mathbf{x}_i - \mathbf{q}\|_2 \right).$$

To increase its performance, the first point, which was chosen uniformly at random, is usually discarded in the end and replaced by a new point chosen via the criteria outlined above.

## 3 Archetypal Analysis++

The idea of the proposed Archetypal Analysis++ initialization procedure is very similar to the one from  $k$ -means++. We begin with choosing the first archetype uniformly at random. The second archetype is chosen according to a distribution that assigns probabilities proportional to the distance from the first archetype, i.e.,  $p(\mathbf{x}) \propto \|\mathbf{x} - \mathbf{z}_1\|_2^2$ . The remaining  $k - 2$  archetypes are chosen according to a probability distribution where the probability of choosing a point  $\mathbf{x}$  is proportional to the minimum distance to the convex hull of the already chosen archetypes, i.e.,  $p(\mathbf{x}) \propto \min_{\mathbf{q} \in \text{conv}(\{\mathbf{z}_1, \dots, \mathbf{z}_k\})} \|\mathbf{x} - \mathbf{q}\|_2^2$ . This procedure is depicted in Figure 2 and outlined in Algorithm 3.

With every additional point sampled, the convex hull of the initialized factors, i.e.,  $\text{conv}(\mathcal{Z})$ , expands. This is because selecting a point outside the convex hull of  $\mathcal{Z}$ , i.e., a point in  $\{\mathbf{x} \in \mathcal{X} \mid \mathbf{x} \notin \text{conv}(\mathcal{Z})\}$ , is by definition not contained in the convex hull of  $\mathcal{Z}$  and hence expands it. In contrast, a point within the convex hull of  $\mathcal{Z}$  would not increase its volume but has zero probability of being selected. However, selecting a new point can make a previously selected point redundant, i.e., it then lies in the convex hull of all selected initial archetypes and does not help to increase it. However, this is not a problem, as our empirical evaluation later shows.

Note that line 6 of Algorithm 3 solves the same optimization problem as line 5 in Algorithm 2. Thus, parts of the archetypal analysis implementations can be re-used, simplifying the implementation of AA++. Besides, AA++ has no hyperparameters, and line 6 can be trivially parallelized.

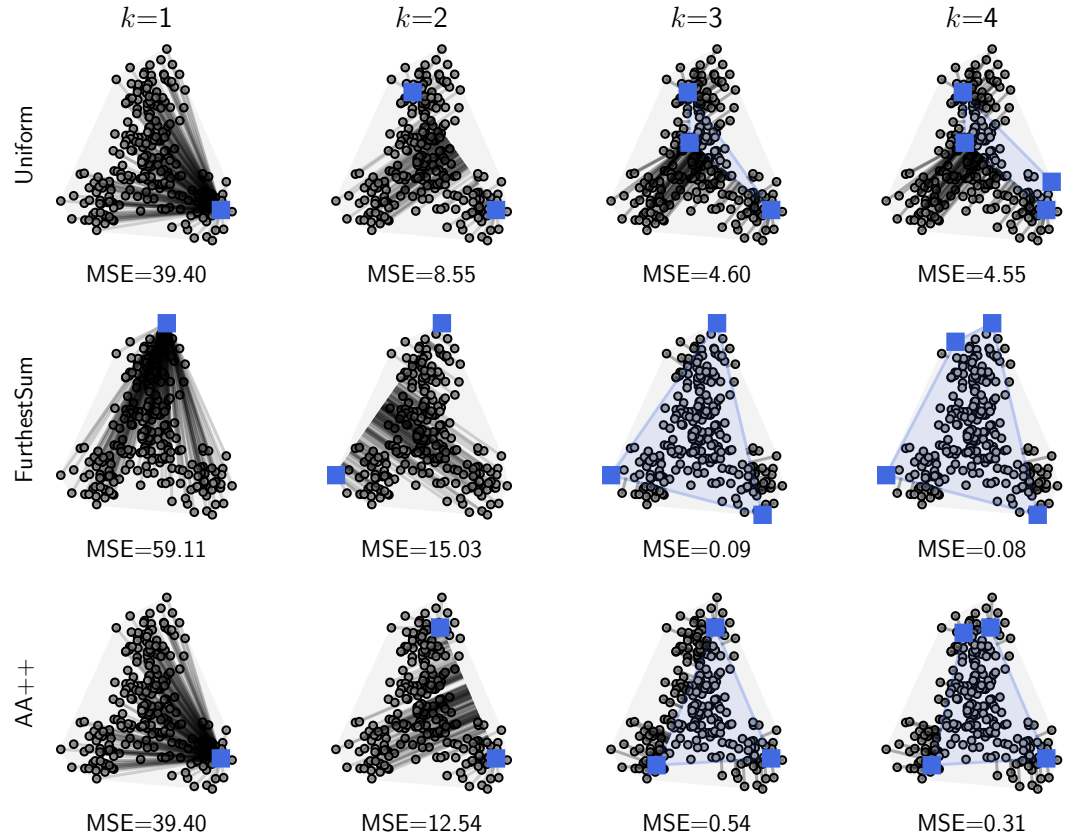


**Figure 2.** A comparison of Uniform, FurthestSum, and the proposed AA++ when consecutively initializing  $k = 4$  archetypes.

### 3.1 Theoretical Analysis

We first show that by adding a new archetype  $z$  to the set of archetypes  $\mathcal{Z}$  in the while loop of AA++ in Algorithm 3, the objective function decreases or remains unchanged.

**Lemma 3.1.** *Adding a point  $x$  to the set of archetypes  $\mathcal{Z}$  either decreases the objective function or leaves it unchanged.*

*Proof.* Let  $\mathcal{P} = \text{conv}(\mathcal{Z})$  be the polytope corresponding to the convex hull of the archetypes. There are only three scenarios. First, the added point  $x$  lies within  $\mathcal{P}$ . Then,  $\mathcal{P}$  remains unchanged and so do the projections of the points outside of  $\mathcal{P}$ . Hence, the value of the objective function remains unchanged. Second, the added point  $x$  lies outside of  $\mathcal{P}$  and  $x$  is the only point projected on that face of  $\mathcal{P}$ . Then,  $x$  increases the volume of the convex hull but the projections and thus the value of the objective function remain the same. Third, the added point  $x$  lies outside of  $\mathcal{P}$  and there are other points that lie on the same face of  $\mathcal{P}$  as  $x$ . Then,  $x$  increases the volume of the convex hull and thus decreases the projections of the other points that lie on the same face. Hence, the value of the objective function decreases.  $\square$

Note that using a random initialization samples archetypes that fall in all three categories mentioned in the proof. In comparison, the proposed approach only considers points from the latter two categories when adding a new point.

We now show that sampling  $k$  points according to our data-dependent sampling procedure results in a larger (in terms of volume) convex hull of sampled points compared to a uniform sample in expectation. Thus, the projection of points onto this convex hull (cost) is expected to be smaller.

**Proposition 3.2.** *AA++ (Algorithm 3) grows the volume of the convex hull of  $\mathcal{Z}$  faster than a uniform initialization in expectation.*

The proof of Proposition 3.2 can be found in the appendix.

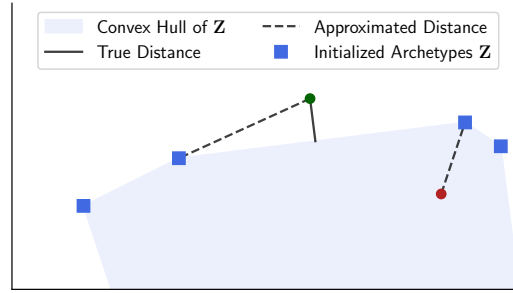


**Figure 3.** Approximation of the distance function. The true distance of the green point is depicted using a solid line whereas the approximation is shown as a (larger) dashed line. The red point has no distance to the convex hull, but the approximation yields a positive distance.

### 3.2 Complexity Analysis

The proposed initialization strategy outlined in Algorithm 3 selects the first archetype uniformly at random. The remaining  $k - 1$  archetypes are chosen according to a probability proportional to the squared distance between the candidate point and the convex hull of the already chosen archetypes. To compute this projection, a quadratic program (QP) has to be solved. Thus, the complexity of Algorithm 3 is  $\mathcal{O}(n \cdot k \cdot \text{QP})$ . It depends not only on the size of the data set  $n$  and the number of archetypes  $k$  to be initialized but also on the complexity of solving the quadratic program  $\mathcal{O}(\text{QP})$ , which is often cubic in the number of variables  $k$  (Goldfarb and Liu, 1990).

## 4 Approximating the Archetypal Analysis++ Initialization

The proposed initialization procedure AA++ has to solve  $n \cdot k$  quadratic programs, which can be time-consuming. Thus, we provide two strategies to approximate the initialization procedure.

### 4.1 Approximating the Distance Computation

Mair and Brefeld (2019) show that the objective function of  $k$ -means upper bounds the objective of archetypal analysis, which is due to the per-point projections, i.e.,

$$\min_{\mathbf{q} \in \text{conv}(\mathcal{Z})} \|\mathbf{x} - \mathbf{q}\|_2^2 \leq \min_{\mathbf{q} \in \mathcal{Z}} \|\mathbf{x} - \mathbf{q}\|_2^2$$

for a set of clusters/archetypes  $\mathcal{Z}$ . Since the computationally most expensive operation in the proposed Algorithm 3 is the projection onto the convex hull in line 6, it can be approximated by the distance to the closest point within the already chosen archetypes. See Figure 3 for an example. Note that the distance is then always over-estimated and even points within the convex hull of the already chosen points might have a distance, although the projection should have a length of zero. This is depicted in Figure 3 for the red point. Following this approach boils down to the  $k$ -means++ initialization procedure. Hence, the new complexity is  $\mathcal{O}(n \cdot k \cdot d)$ , thus avoiding the cost of solving the QP.

### 4.2 Approximating the Sampling Procedure

Another approach is to approximate the sampling procedure by avoiding to consider every of the  $n$  data points which is especially beneficial in large-scale scenarios. To initialize  $k$ -means++ in sublinear time, Bachem et al. (2016) leverage a Markov Chain Monte Carlo (MCMC) sampling procedure. This procedure is based on the Metropolis-Hastings algorithm (Hastings, 1970) with an independent and uniform proposal distribution. We adapt this idea for AA++ as follows. The first archetype is still sampled uniformly at random. For every following archetype, a Markov chain of length  $m \ll n$  is constructed iteratively. We begin by sampling an initial point  $\mathbf{x}_i$ . Then, in every step of the chain, we sample a candidate point  $\mathbf{x}_j$  and compute the acceptance probability, which is given by

$$\pi = \min \left( 1, \frac{\min_{\mathbf{q} \in \text{conv}(\mathcal{Z})} \|\mathbf{x}_j - \mathbf{q}\|_2^2}{\min_{\mathbf{q} \in \text{conv}(\mathcal{Z})} \|\mathbf{x}_i - \mathbf{q}\|_2^2} \right).$$



---

**Algorithm 4** AA++ Monte Carlo Initialization

---

```
1: Input: Set of  $n$  data points  $\mathcal{X}$ , number of archetypes  $k$ , chain length  $m$ 
2: Output: Initial set of archetypes  $\mathcal{Z}$ 
3: Sample index  $i$  uniformly at random from  $[n]$ , i.e.,
   using  $p(i) = n^{-1}$ 
4: Append  $\mathbf{x}_i$  to  $\mathcal{Z}$ 
5: while  $|\mathcal{Z}| < k$  do
6:   Sample  $i$  uniformly at random from  $[n]$ , i.e.,
     using  $p(i) = n^{-1}$ 
7:   Compute the distance to the convex hull, i.e.,
      $d_i^2 = \min_{\mathbf{q} \in \text{conv}(\mathcal{Z})} \|\mathbf{x}_i - \mathbf{q}\|_2^2$ 
8:   for  $l = 2, 3, \dots, m$  do
9:     Sample  $j$  uniformly at random from  $[n]$ , i.e.,
       using  $p(j) = n^{-1}$ 
10:    Compute the distance to the convex hull, i.e.,
      $d_j^2 = \min_{\mathbf{q} \in \text{conv}(\mathcal{Z})} \|\mathbf{x}_j - \mathbf{q}\|_2^2$ 
11:    if  $d_j^2/d_i^2 > \text{Unif}(0, 1)$  then
12:       $i = j$ 
13:       $d_i^2 = d_j^2$ 
14:    end if
15:  end for
16:  Append  $\mathbf{x}_i$  to  $\mathcal{Z}$ 
17: end while
```

---

With probability  $\pi$ , we update the current state from  $\mathbf{x}_i$  to  $\mathbf{x}_j$ , otherwise we keep  $\mathbf{x}_i$ . After  $m$  steps, we add the current  $\mathbf{x}_i$  as the next archetype to the set of initial archetypes  $\mathcal{Z}$ . This approach is summarized in Algorithm 4, and the complexity of this strategy is  $\mathcal{O}(m \cdot k \cdot \text{QP})$ .

Bachem et al. (2016) also provide a theoretical result that bounds the error in terms of the total variation distance of the approximate sampling distribution to the true sampling distribution. Here,  $\|p - q\|_{\text{TV}}$  denotes the total variation distance between two distributions  $p$  and  $q$  which is defined as

$$\|p - q\|_{\text{TV}} = \frac{1}{2} \sum_{\mathbf{x} \in \Omega} |p(\mathbf{x}) - q(\mathbf{x})|,$$

where  $\Omega$  is a finite sample space on which both distributions are defined on. The following bound on the error shows that the longer the chain length  $m$ , the smaller the error  $\epsilon$ .

**Theorem 4.1** (Bachem et al. (2016)). *Let  $k > 0$  and  $0 < \epsilon < 1$ . Let  $p_{++}$  be the probability distribution over  $\mathcal{Z}$  defined by using AA++ (Algorithm 3) and  $p_{\text{MCMC}}$  be the probability distribution over  $\mathcal{Z}$  defined by using AA++MC (Algorithm 4). Then,*

$$\|p_{\text{MCMC}} - p_{++}\|_{\text{TV}} \leq \epsilon$$

for a chain length  $m = \mathcal{O}(\gamma' \log \frac{k}{\epsilon})$ , where

$$\gamma' = \max_{\mathcal{Z} \subset \mathcal{X}, |\mathcal{Z}| \leq k} \max_{\mathbf{x} \in \mathcal{X}} n \frac{d(\mathbf{x}, \mathcal{Z})^2}{\sum_{\mathbf{x}' \in \mathcal{X}} d(\mathbf{x}', \mathcal{Z})^2},$$

and  $d(\mathbf{x}, \mathcal{Z})^2 = \min_{\mathbf{q} \in \text{conv}(\mathcal{Z})} \|\mathbf{x} - \mathbf{q}\|_2^2$ .

Note that  $\gamma'$  is a property of the data set.

## 5 Experiments

### Data

We use the following six real-world data sets of varying sizes and dimensionalities. Additional eight real-world data sets are considered in the appendix.

A first large data set is *Covertypes* (Blackard and Dean, 1999), which consists of  $n = 581,012$  instances in  $d = 54$  dimensions. The *Ijcnn1* data set has  $n = 49,990$  points in  $d = 22$  dimensions and was used in the IJCNN 2001 neural network competition.<sup>1</sup> We employ the same pre-processing as Chang and Lin (2001). *KDD-Protein*<sup>2</sup> has  $n = 145,751$  data points, each represented with  $d = 74$  dimensions measuring the match between a protein and a native sequence. The data set *Pose* is a subset of the Human3.6M data set (Catalin Ionescu, 2011; Ionescu et al., 2014). *Pose* was used in the ECCV 2018 PoseTrack Challenge and deals with 3D human pose estimation.<sup>3</sup> Each of the  $n = 35,832$  poses is represented as 3D coordinates of 16 joints. Thus, the problem is 48-dimensional. Another larger data set we use is a subset of the Million Song Dataset (Bertin-Mahieux et al., 2011), which is called *Song*. It has  $n = 515,345$  data points in  $d = 90$  dimensions. Furthermore, we utilize the *MNIST* (LeCun et al., 2010) data of size  $n = 60,000$ , which contains gray-scale images size  $28 \times 28$  showing handwritten digits, thus having ten classes. We use the subset of images showing the digit 4. This subset has  $n = 5,842$  data points in  $d = 784$  dimensions.

### Data Pre-processing

We apply pre-processing to avoid numerical problems during learning. In total, we consider two different approaches: (i) *CenterAndMaxScale*, in which the data set is first centered and then the data matrix is divided by the largest element, and (ii) *Standardization* which also centers the data set but then divides every dimension by its standard deviation. Results on *CenterAndMaxScale* are presented in the main paper, while results on *Standardization* are presented in the appendix.

### Baselines

We compare our proposed initialization strategy *AA++* against a *Uniform* subsample of all data points, *FurthestFirst* (Gonzalez, 1985; Hochbaum and Shmoys, 1985), and *FurthestSum* (Mørup and Hansen, 2010, 2012). In addition, we evaluate two approximations, the first of which is equivalent to *k-means++* and the second one, which is *AA++MC*. For the latter, we evaluate 1%, 5%, 10%, and 20% of the data set size as chain lengths  $m$ . Note that by *k-means++* we only refer to the initialization strategy.

### Setup

For various numbers of archetypes  $k$  depending on the data set, we initialize archetypal analysis according to each of the baseline strategies and compute the Mean Squared Error (MSE), i.e., the objective in Equation (2) normalized by  $n^{-1}$ . In addition, we perform a fixed number of ten iterations of archetypal analysis based on those initializations. Here, we use the vanilla version of archetypal analysis according to Cutler and Breiman (1994). For the optimization problem within *AA++*, we utilize the non-negative least squares (NNLS) method (Lawson and Hanson, 1995) and enforce the summation constraint by adding another equation in the linear system.

We compute statistics over 50 seeds, except for the larger data sets ( $n > 500,000$ ) for which we only use 15 seeds. We report on median performances and depict the 75% and 25% quantiles. Furthermore, we track the time it takes to initialize the archetypes. The code is implemented in Python using numpy (Harris et al., 2020).<sup>4</sup> All experiments run on an Intel Xeon machine with 28 cores with 2.60 GHz and 256 GB of memory.

### Results on MNIST

We first analyze the behavior of the most commonly used baselines *Uniform* and *FurthestSum*, and compare it to our proposed *AA++* strategy. To do so, we use the MNIST data restricted to the digit 4 and visualize the  $k = 3$  chosen initial archetypes  $z_1, z_2, z_3$  per initialization method in Figure 4. We can see that *Uniform* picks three very similar samples, whereas *FurthestSum* rather chooses outliers. In comparison, *AA++* yields a selection with more variation yet without outliers. This is also reflected in the MSE right after initialization. Here, *AA++* yields the lowest MSE and thus explains the data best.

Figure 5 shows the MSE right after initialization as a small straight line on the left-hand-side and then ten iterations of archetypal analysis for  $k = 3$  and  $k = 9$  archetypes. Note that the y-axis is in log-scale and that the lines reflect median values over 50 seeds. In both cases, *FurthestSum* yields the

<sup>1</sup><https://www.csie.ntu.edu.tw/~cjlin/libsvmtools/datasets/>

<sup>2</sup><http://osmot.cs.cornell.edu/kddcup/datasets.html>

<sup>3</sup>[http://vision.imar.ro/human3.6m/challenge\\_open.php](http://vision.imar.ro/human3.6m/challenge_open.php)

<sup>4</sup>We will release the code on github after the paper is accepted.



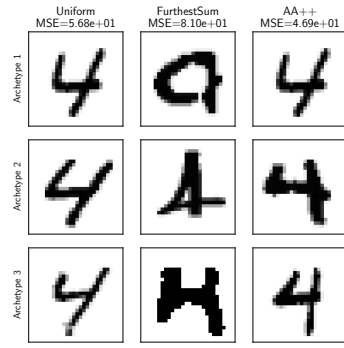


**Figure 4.** Three initial archetypes on MNIST restricted to the digit 4 chosen by two baselines and our proposed AA++ method.

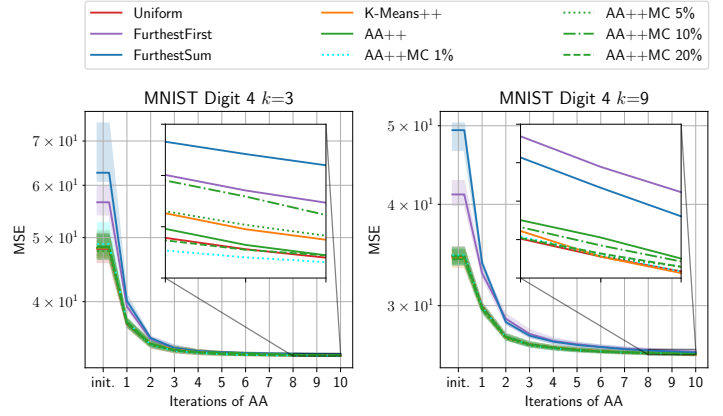


**Figure 5.** Optimization trajectories for  $k = 3, 9$  on MNIST restricted to the digit 4. The part from iterations 8 to 10 is enlarged.

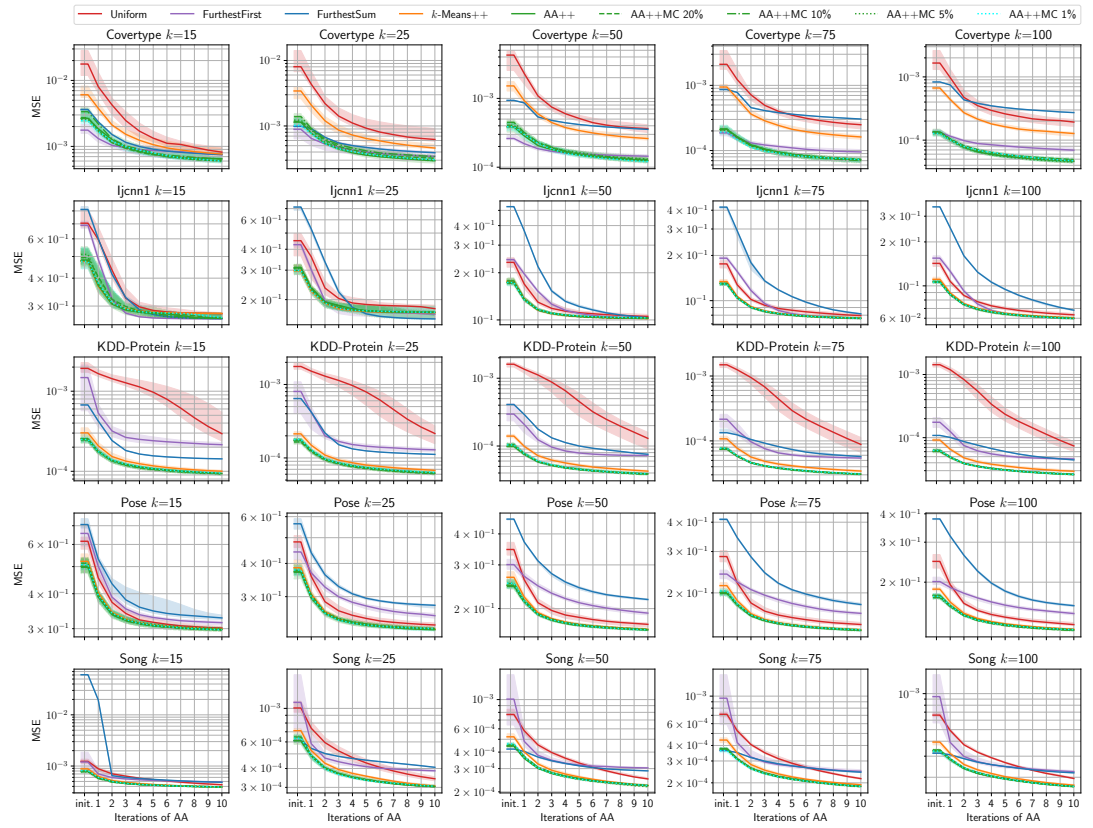


**Figure 6.** Results on Covertypes, Ijcnn1, KDD-Protein, Pose, and Song.

worst initialization and also performs worse than most of its competitors during optimization, while AA++ and Uniform perform much better.

### Performance Results

We evaluate the initialization strategies on five further data sets to get a better impression of the performance. Figure 6 depicts the results on Covertypes, Ijcnn1, KDD-Protein, Pose, and Song. Although being the most commonly used initialization methods, Uniform (red line) and FurthestSum (blue line) often yield the worst initializations which can be seen by the short straight line on the left-hand-side. During the first ten iterations of archetypal analysis, the error decreases. However, there is frequently

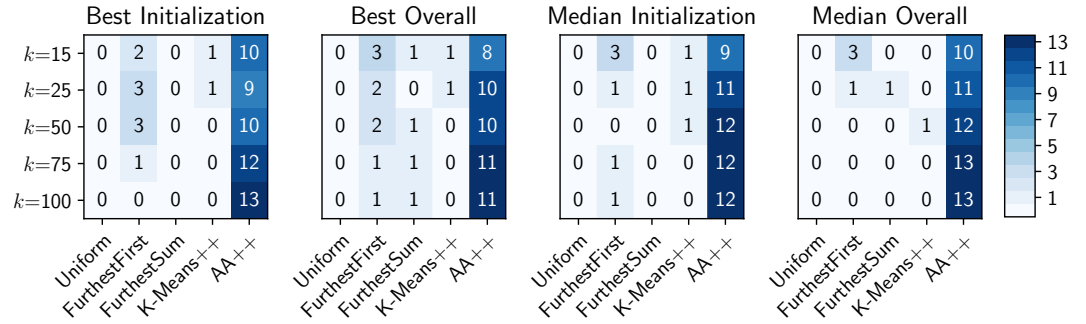


**Figure 7.** Aggregated statistics over 13 data sets (five data sets from above excluding MNIST and eight data sets from the appendix). Each table shows how often each initialization method yields the best result for various settings of  $k$  under different settings. Best refers to the lowest single seed and median refers to the median over many seeds. We report on the performance after initialization and overall during the optimization.

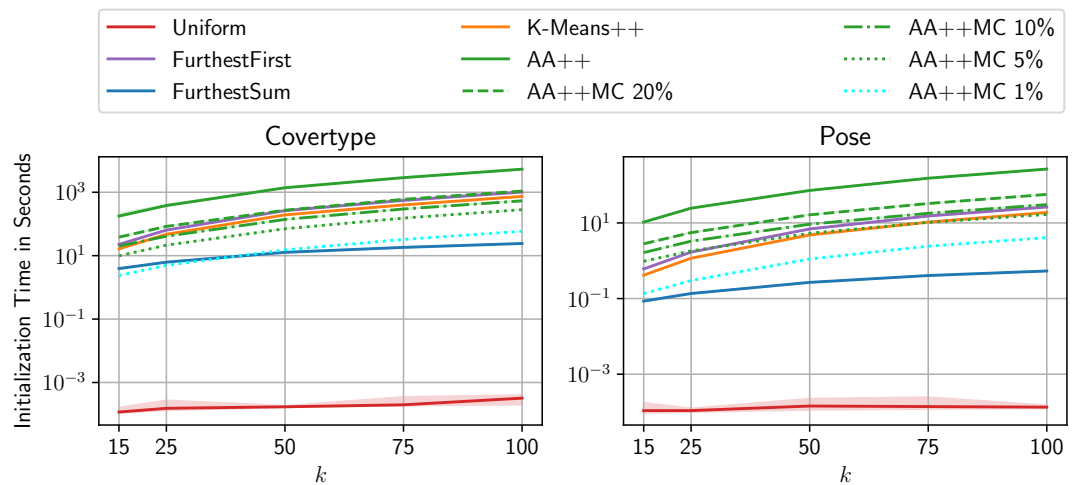


**Figure 8.** The median time it takes to initialize archetypal analysis.

a significant performance gap between Uniform and FurthestSum when compared to AA++ (green line), especially for Covertypes, KDD-Protein, and Pose. The baseline  $k$ -means++ (orange line), which can be seen as an approximation to AA++, often performs similar to AA++ and almost always better than FurthestFirst (purple line), except on Covertypes. As for the Monte Carlo approximations of AA++ using 1%, 5%, 10%, and 20% of the data set size as chain lengths  $m$ , we can see that they approximate AA++ sufficiently well on these data sets. Overall, our proposed AA++ initialization performs best in almost all cases.

This is confirmed in the aggregated statistics in Figure 7. Each table shows how often each initialization method (approximations excluded) performs best on the evaluated data sets. In total, we consider 13 data sets: all previously introduced data sets excluding MNIST and eight data sets which are considered in the appendix. Thus, 13 is the highest and best number that can appear in those tables. Within Figure 7, *best* refers to the lowest outcome among all seeds, and *median* refers to the median over all seeds per method. Besides, *initialization* only considers the performance after initialization, whereas *overall* reflects the best performance across iterations of AA, which is typically at the last iteration. Once again, AA++ clearly yields the best results in all scenarios, especially for larger values of  $k$ .

### Timing Results

Unfortunately, the increase in performance comes at a cost. Figure 8 shows the time needed for initializing the archetypes on the Covertypes and Pose data sets for various choices of  $k$ . As expected,

the fastest-performing method is Uniform since it uses no information about the data except the number of data points. FurthestSum is slower than Uniform, and the proposed approach AA++ is consistently the slowest. However, note that initializing  $k$  points is still much cheaper than running  $k$  AA iterations. Using the MCMC-based approximation reduces the initialization time of AA++ drastically, e.g., on Coverttype, AA++MC using 1% of the data points as the chain length  $m$  takes approximately as much time as FurthestSum.

### Influence of the Pre-processing Scheme

A surprising finding is that FurthestSum is especially sensitive to the pre-processing scheme, as shown in Figure 11 in the appendix. Standardization clearly degrades the performance of FurthestSum but does not affect AA++ and its approximations.

## 6 Related Work

Other variants exist besides the classical archetypal analysis (Cutler and Breiman, 1994). Moving archetypes (Cutler and Stone, 1997) defines AA for moving targets. There are adaptations of archetypal analysis for missing data (Epifanio et al., 2020) and interval data (D’Esposito et al., 2012), and probabilistic archetypal analysis (Seth and Eugster, 2016) rephrases the factorization problem in a probabilistic way. More recently, approaches based on deep learning have been considered Keller et al. (2019); van Dijk et al. (2019); Keller et al. (2021). For those, the initialization of archetypes is irrelevant, as considered in this paper. Furthermore, archetypoid analysis (Vinué et al., 2015) restricts the archetypes to be data points instead of convex combinations of data points. Hence, the idea is similar to  $k$ -medoids (Kaufman and Rousseeuw, 1990) and intends to add more interpretability. Note that AA++ can also be used as an initialization for archetypoid analysis.

Suleman (2017) stresses that an improper initialization of archetypal analysis is problematic and that the FurthestSum method is prone to selecting redundant archetypes, especially when having many archetypes. This is contradicted by our experiments, which show that FurthestSum’s problem is rather the poor choice of boundary points. Nascimento and Madaleno (2019) consider an anomalous pattern initialization algorithm for initializing archetypal analysis. However, their focus was on inferring the number of archetypes  $k$  and then using archetypal analysis for fuzzy clustering.

Less common initialization strategies for archetypal analysis include  $k$ -means, as used by Han et al. (2022), and a coresets (Mair and Brefeld, 2019), as used by Black et al. (2022) and Chapman et al. (2022). Note that the coresets was proposed as a way to condense the data set into a smaller set for a more efficient training of archetypal analysis rather than as a way for initializing it. Hence, we don’t compare to it.

For the related non-negative matrix factorization (NMF) (Lee and Seung, 1999) problem, several initialization techniques based on randomization, other low-rank decompositions, clusterings, heuristics, and even learned approaches (Sjölund and Bänkestad, 2022) are used. A summary of various NMF initialization methods is provided by Esposito (2021). Among the considered baselines in this paper, all are randomized. However, FurthestSum can be seen as a heuristic, and FurthestFirst and  $k$ -means++ can be classified as clusterings. The proposed AA++ approach is randomized just as Uniform, with the difference that AA++ is data-dependent and Uniform is data-independent.

## 7 Conclusion

We introduced archetypal analysis++ (AA++), an initialization method for archetypal analysis inspired by  $k$ -means++. The proposed method does not have any hyperparameters and is straightforward to implement, as it re-uses already existing subroutines of any implementation of archetypal analysis. Furthermore, we showed that the  $k$ -means++ initialization method can be seen as an approximation to AA++, and we also proposed an MCMC approximation of AA++ to reduce the computational effort. We empirically verified, for two pre-processing schemes, that AA++ essentially consistently outperforms all baselines, including the most frequently used ones, namely Uniform and FurthestSum, on 13 real-world data sets of varying sizes and dimensionalities.

## References

- Abrol, V. and Sharma, P. (2020). A geometric approach to archetypal analysis via sparse projections. In *Proceedings of International Conference on Machine Learning*, pages 42–51. PMLR.
- Arthur, D. and Vassilvitskii, S. (2007). K-means++: The advantages of careful seeding. In *Proceedings of the Eighteenth Annual ACM-SIAM Symposium on Discrete Algorithms*, SODA '07, pages 1027–1035. Society for Industrial and Applied Mathematics.
- Bachem, O., Lucic, M., Hassani, S. H., and Krause, A. (2016). Approximate k-means++ in sublinear time. In *Thirtieth AAAI conference on artificial intelligence*.
- Bauckhage, C., Kersting, H., Thureau, C., et al. (2015). Archetypal analysis as an autoencoder. In *Workshop New Challenges in Neural Computation*.
- Bauckhage, C. and Thureau, C. (2009). Making archetypal analysis practical. In *Joint Pattern Recognition Symposium*, pages 272–281. Springer.
- Beck, C., Kunze, A., and Zosso, D. (2022). Archetypal analysis for neuronal clique detection in low-rate calcium fluorescence imaging. In *Proceedings of the 44th Annual International Conference of the IEEE Engineering in Medicine & Biology Society*, pages 162–166. IEEE.
- Bertin-Mahieux, T., Ellis, D. P., Whitman, B., and Lamere, P. (2011). The million song dataset. In *Proceedings of the 12th International Conference on Music Information Retrieval*.
- Black, A. S., Monselesan, D. P., Risbey, J. S., Sloyan, B. M., Chapman, C. C., Hannachi, A., Richardson, D., Squire, D. T., Tozer, C. R., and Trendafilov, N. (2022). Archetypal analysis of geophysical data illustrated by sea surface temperature. *Artificial Intelligence for the Earth Systems*, 1(3):e210007.
- Blackard, J. A. and Dean, D. J. (1999). Comparative accuracies of artificial neural networks and discriminant analysis in predicting forest cover types from cartographic variables. *Computers and electronics in agriculture*, 24(3):131–151.
- Brooks, T. F., Pope, D. S., and Marcolini, M. A. (1989). Airfoil self-noise and prediction.
- Catalin Ionescu, Fuxin Li, C. S. (2011). Latent structured models for human pose estimation. In *International Conference on Computer Vision*.
- Chang, C.-c. and Lin, C.-J. (2001). IJCNN 2001 challenge: Generalization ability and text decoding. In *Proceedings of International Joint Conference on Neural Networks*, volume 2, pages 1031–1036. IEEE.
- Chapman, C., Monselesan, D., Risbey, J., Feng, M., and Sloyan, B. (2022). Large-scale drivers of marine heatwaves revealed by archetype analysis.
- Chen, Y., Mairal, J., and Harchaoui, Z. (2014). Fast and robust archetypal analysis for representation learning. In *Proceedings of the IEEE Conference on Computer Vision and Pattern Recognition*, pages 1478–1485.
- Cutler, A. and Breiman, L. (1994). Archetypal analysis. *Technometrics*, 36(4):338–347.
- Cutler, A. and Stone, E. (1997). Moving archetypes. *Physica D: Nonlinear Phenomena*, 107(1):1–16.
- Damle, A. and Sun, Y. (2017). A geometric approach to archetypal analysis and nonnegative matrix factorization. *Technometrics*, 59(3):361–370.
- D’Esposito, M. R., Palumbo, F., and Ragozini, G. (2012). Interval archetypes: a new tool for interval data analysis. *Statistical Analysis and Data Mining: The ASA Data Science Journal*, 5(4):322–335.
- Dua, D. and Graff, C. (2017). UCI machine learning repository.
- Dulá, J. H. and López, F. J. (2012). Competing output-sensitive frame algorithms. *Computational Geometry*, 45(4):186–197.

- Epifanio, I., Ibáñez, M. V., and Simó, A. (2020). Archetypal analysis with missing data: see all samples by looking at a few based on extreme profiles. *The American Statistician*, 74(2):169–183.
- Esposito, F. (2021). A review on initialization methods for nonnegative matrix factorization: towards omics data experiments. *Mathematics*, 9(9):1006.
- Eugster, M. J. and Leisch, F. (2011). Weighted and robust archetypal analysis. *Computational Statistics & Data Analysis*, 55(3):1215–1225.
- Gimbernat-Mayol, J., Dominguez Mantes, A., Bustamante, C. D., Mas Montserrat, D., and Ioannidis, A. G. (2022). Archetypal analysis for population genetics. *PLoS Computational Biology*, 18(8):e1010301.
- Goldfarb, D. and Liu, S. (1990). An  $\mathcal{O}(n^3L)$  primal interior point algorithm for convex quadratic programming. *Mathematical programming*, 49(1):325–340.
- Gonzalez, T. F. (1985). Clustering to minimize the maximum intercluster distance. *Theoretical Computer Science*, 38:293–306.
- Han, R., Osting, B., Wang, D., and Xu, Y. (2022). Probabilistic methods for approximate archetypal analysis. *Information and Inference: A Journal of the IMA*.
- Hannachi, A. and Trendafilov, N. (2017). Archetypal analysis: Mining weather and climate extremes. *Journal of Climate*, 30(17):6927–6944.
- Harris, C. R., Millman, K. J., van der Walt, S. J., Gommers, R., Virtanen, P., Cournapeau, D., Wieser, E., Taylor, J., Berg, S., Smith, N. J., Kern, R., Picus, M., Hoyer, S., van Kerkwijk, M. H., Brett, M., Haldane, A., del Río, J. F., Wiebe, M., Peterson, P., Gérard-Marchant, P., Sheppard, K., Reddy, T., Weckesser, W., Abbasi, H., Gohlke, C., and Oliphant, T. E. (2020). Array programming with NumPy. *Nature*, 585(7825):357–362.
- Hart, Y., Sheftel, H., Hausser, J., Szekely, P., Ben-Moshe, N. B., Korem, Y., Tandler, A., Mayo, A. E., and Alon, U. (2015). Inferring biological tasks using pareto analysis of high-dimensional data. *Nature Methods*, 12(3):233–235.
- Hastings, W. (1970). Monte Carlo sampling methods using Markov chains and their applications. *Biometrika*, 57(1):97–109.
- Hinrich, J. L., Bardenfleth, S. E., Røge, R. E., Churchill, N. W., Madsen, K. H., and Mørup, M. (2016). Archetypal analysis for modeling multisubject fMRI data. *IEEE Journal of Selected Topics in Signal Processing*, 10(7):1160–1171.
- Hochbaum, D. S. and Shmoys, D. B. (1985). A best possible heuristic for the k-center problem. *Mathematics of Operations Research*, 10(2):180–184.
- Ionescu, C., Papava, D., Olaru, V., and Sminchisescu, C. (2014). Human3.6M: Large Scale Datasets and Predictive Methods for 3D Human Sensing in Natural Environments. *IEEE Transactions on Pattern Analysis and Machine Intelligence*.
- Kaufman, L. and Rousseeuw, P. J. (1990). *Partitioning Around Medoids (Program PAM)*. Wiley And Sons.
- Keller, S. M., Samarin, M., Arend Torres, F., Wieser, M., and Roth, V. (2021). Learning extremal representations with deep archetypal analysis. *International Journal of Computer Vision*, 129(4):805–820.
- Keller, S. M., Samarin, M., Wieser, M., and Roth, V. (2019). Deep archetypal analysis. In *German Conference on Pattern Recognition*, pages 171–185. Springer.
- Krohne, L. G., Wang, Y., Hinrich, J. L., Moerup, M., Chan, R. C., and Madsen, K. H. (2019). Classification of social anhedonia using temporal and spatial network features from a social cognition fMRI task. *Human Brain Mapping*, 40(17):4965–4981.



- Lawson, C. L. and Hanson, R. J. (1995). *Solving least squares problems*, volume 15. SIAM.
- LeCun, Y., Cortes, C., and Burges, C. (2010). MNIST handwritten digit database. *ATT Labs [Online]*. Available: <http://yann.lecun.com/exdb/mnist>, 2.
- Lee, D. D. and Seung, H. S. (1999). Learning the parts of objects by non-negative matrix factorization. *Nature*, 401(6755):788–791.
- Lloyd, S. (1982). Least squares quantization in PCM. *IEEE Transactions on Information Theory*, 28(2):129–137.
- Mair, S., Boubekki, A., and Brefeld, U. (2017). Frame-based data factorizations. In *International Conference on Machine Learning*, pages 2305–2313. PMLR.
- Mair, S. and Brefeld, U. (2019). Coresets for archetypal analysis. *Advances in Neural Information Processing Systems*, 32.
- Mei, J., Wang, C., and Zeng, W. (2018). Online dictionary learning for approximate archetypal analysis. In *Proceedings of the European Conference on Computer Vision*, pages 486–501.
- Mørup, M. and Hansen, L. K. (2010). Archetypal analysis for machine learning. In *Proceedings of IEEE International Workshop on Machine Learning for Signal Processing*, pages 172–177. IEEE.
- Mørup, M. and Hansen, L. K. (2012). Archetypal analysis for machine learning and data mining. *Neurocomputing*, 80:54–63.
- Nascimento, S. and Madaleno, N. (2019). Unsupervised initialization of archetypal analysis and proportional membership fuzzy clustering. In *International Conference on Intelligent Data Engineering and Automated Learning*, pages 12–20. Springer.
- Olsen, A. S., Høegh, R. M., Hinrich, J. L., Madsen, K. H., and Mørup, M. (2022). Combining electro-and magnetoencephalography data using directional archetypal analysis. *Frontiers in Neuroscience*, 16.
- Ostrovsky, R., Rabani, Y., Schulman, L. J., and Swamy, C. (2013). The effectiveness of lloyd-type methods for the k-means problem. *Journal of the ACM*, 59(6):1–22.
- Pace, R. K. and Barry, R. (1997). Sparse spatial autoregressions. *Statistics & Probability Letters*, 33(3):291–297.
- Seth, S. and Eugster, M. J. (2015). Archetypal analysis for nominal observations. *IEEE Transactions on Pattern Analysis and Machine Intelligence*, 38(5):849–861.
- Seth, S. and Eugster, M. J. (2016). Probabilistic archetypal analysis. *Machine Learning*, 102(1):85–113.
- Sjölund, J. and Bänkestad, M. (2022). Graph-based neural acceleration for nonnegative matrix factorization. *arXiv preprint arXiv:2202.00264*.
- Suleman, A. (2017). On ill-conceived initialization in archetypal analysis. *Advances in Data Analysis and Classification*, 11(4):785–808.
- Thøgersen, J. C., Mørup, M., Damkiær, S., Molin, S., and Jelsbak, L. (2013). Archetypal analysis of diverse pseudomonas aeruginosatrascriptomes reveals adaptation in cystic fibrosis airways. *BMC Bioinformatics*, 14(1):1–15.
- Udell, M., Horn, C., Zadeh, R., Boyd, S., et al. (2016). Generalized low rank models. *Foundations and Trends in Machine Learning*, 9(1):1–118.
- Uzilov, A. V., Keegan, J. M., and Mathews, D. H. (2006). Detection of non-coding rnas on the basis of predicted secondary structure formation free energy change. *BMC Bioinformatics*, 7(1):1–30.
- van Dijk, D., Burkhardt, D. B., Amodio, M., Tong, A., Wolf, G., and Krishnaswamy, S. (2019). Finding archetypal spaces using neural networks. In *Proceedings of IEEE International Conference on Big Data*, pages 2634–2643. IEEE.



Vinué, G., Epifanio, I., and Alemany, S. (2015). Archetypoids: A new approach to define representative archetypal data. *Computational Statistics & Data Analysis*, 87:102–115.

Yeh, I.-C. (1998). Modeling of strength of high-performance concrete using artificial neural networks. *Cement and Concrete Research*, 28(12):1797–1808.

Ziegler, G. (2012). *Lectures on Polytopes*. Graduate Texts in Mathematics. Springer New York.

## A Proof of Proposition 3.2

**Proposition 3.2.** *AA++ (Algorithm 3) grows the volume of the convex hull of  $\mathcal{Z}$  faster than a uniform initialization in expectation.*

Within the proof we use Chebyshev’s sum inequality which states that if  $p_1 \geq p_2 \geq \dots \geq p_n$  and  $r_1 \geq r_2 \geq \dots \geq r_n$ , then  $\frac{1}{n} \sum_{i=1}^n p_i r_i \geq \left(\frac{1}{n} \sum_{i=1}^n p_i\right) \left(\frac{1}{n} \sum_{i=1}^n r_i\right)$ .

*Proof of Proposition 3.2.* Without loss of generality we focus on the two-dimensional setting since similar arguments hold in higher dimensions. AA++ (Algorithm 3) as well as a uniform initialization select the first point uniformly at random. Assume both algorithms start with the same point  $\mathbf{x}$  and call it  $\mathbf{z}_1$ .

After sampling a second point  $\mathbf{z}_2$ , we obtain a line. We first show that the expected length of the line is larger when using AA++. Without loss of generality subtract  $\mathbf{z}_1$  from all  $\mathbf{x}_i$  such that the line is equivalent to the norm of the points. Reorder the points  $\mathbf{x}_i$  according to their norms  $r_i = \|\mathbf{x}_i\|_2$  and let  $p_i = \frac{\|\mathbf{x}_i\|_2^2}{\sum_{j=1}^n \|\mathbf{x}_j\|_2^2}$  be the probability of choosing the point according to AA++. Furthermore, let  $u_i = n^{-1}$  be the probability of choosing the point according to the uniform initialization. Thus,  $p_1 \geq p_2 \geq \dots \geq p_n$  and  $r_1 \geq r_2 \geq \dots \geq r_n$ . Due to Chebyshev’s sum inequality, we obtain

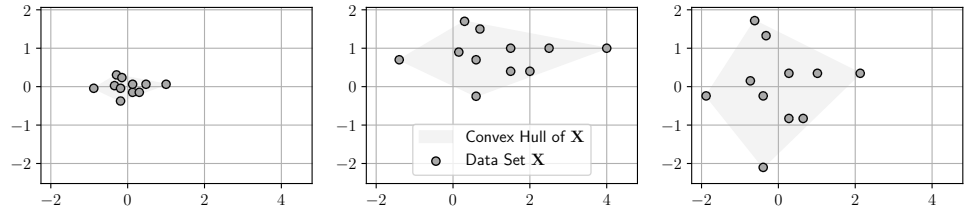
$$\frac{1}{n} \sum_{i=1}^n p_i r_i \geq \left(\frac{1}{n} \sum_{i=1}^n p_i\right) \left(\frac{1}{n} \sum_{i=1}^n r_i\right) \iff \sum_{i=1}^n p_i r_i \geq \frac{1}{n} \sum_{i=1}^n r_i \iff \mathbb{E}_p[\|\mathbf{x}_i\|] \geq \mathbb{E}_u[\|\mathbf{x}_i\|],$$

by using  $\sum_{i=1}^n p_i = 1$  and by multiplying both sides by  $n$ . Hence, showing that the expected length using AA++ is larger than by using a uniform sample.

Now consider the third chosen point which spans  $\text{conv}(\mathcal{Z})$  to a triangle, given the point is not chosen on the line between  $\mathbf{z}_1$  and  $\mathbf{z}_2$ . The growth of volume of the convex hull is thus the area of the triangle, which is  $\frac{1}{2}$  base · height. We already know that the base length is larger for AA++ than for a uniform initialization in expectation. However, we again assume they are the same. Let  $r_i = \min_{\mathbf{q} \in \text{conv}(\mathcal{Z})} \|\mathbf{x}_i - \mathbf{q}\|_2$  be the projecting of each point  $\mathbf{x}_i$  to the line, where  $\mathcal{Z} = \{\mathbf{z}_1, \mathbf{z}_2\}$ , and  $p_i$  the normalized probability of choosing the point according to Algorithm 3, i.e.,  $p_i = \frac{r_i}{\sum_{j=1}^n r_j}$ . Then, by reordering the points as before and applying Chebyshev’s sum inequality again, we have that the expected height is larger for AA++ than for uniform. Hence, the area of the triangle and thus the volume of the convex hull grows faster for AA++. Every further point opens another triangle which contributes in area to the overall volume of the convex hull.  $\square$

## B Pre-processing

In the main body of the paper, we pre-processed the data by first centering the data set and then dividing it by the maximum value. Another frequently used pre-processing scheme is standardization. That is, per dimension, we subtract the mean and divide it by the standard deviation. Since both are linear transformations, they do not change the membership of the points being on the border of the convex hull (Ziegler, 2012). However, the former scheme maintains the shape of the data set in terms of its convex hull, whereas the latter scheme changes it. This is depicted in Figure 9, where the original data is shown in the middle, the pre-processing of the main body of the paper is shown on the left-hand-side and a data standardization is shown on the right-hand-side.



**Appendix B—Figure 9.** Comparison between the two pre-processing approaches. Left: Center data and divide by maximum value. Middle: Original data set. Right: Standardized data set.

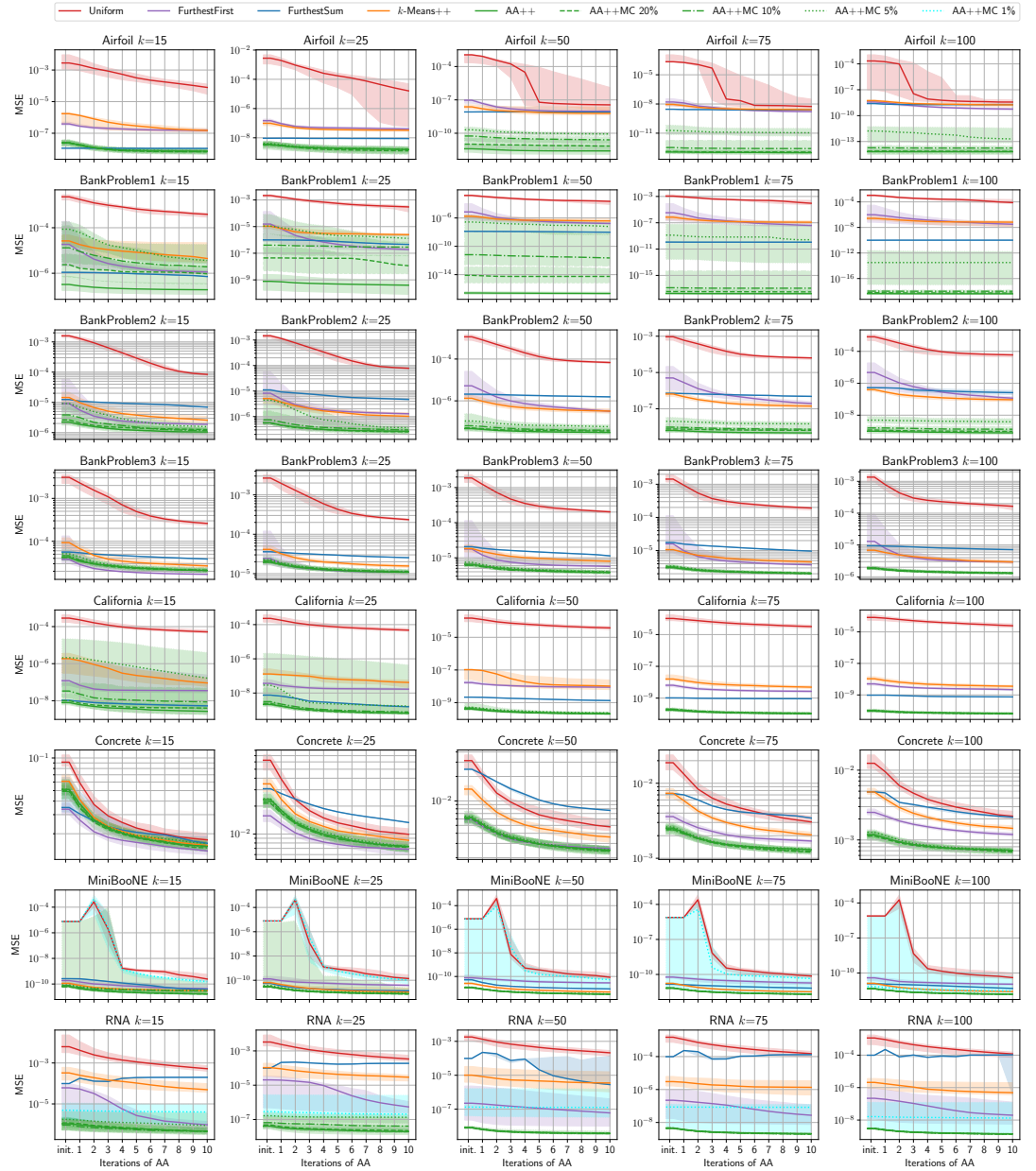
**Appendix C—Table 1.** An overview of the data sets used in this paper. The upper part is considered in the main body of the paper and the lower part is discussed in the appendix.

	Data Set Name	Number of Data Points	Number of Dimensions
Main Paper	Covertypes	581,012	54
	Ijcnn1	49,990	22
	KDD-Protein	145,751	74
	Pose	35,832	48
	Song	515,345	90
	MNIST 4	5,842	784
Appendix	Airfoil	1,503	5
	California Housing	20,640	8
	Concrete	1,030	8
	Banking1	4,971	7
	Banking2	12,456	8
	Banking3	19,939	11
	MiniBooNE	130,064	50
	RNA	488,565	8

## C Results on Additional Data Sets

We further evaluate the initialization methods on the following data sets. *Airfoil* (Brooks et al., 1989) has  $n = 1503$  data points represented in  $d = 5$  dimensions. The *California Housing* (Pace and Barry, 1997) data set has  $n = 20,640$  examples in  $d = 8$  dimensions. *Concrete* (Yeh, 1998) has  $n = 1030$  instances in  $d = 8$  dimensions. The data sets *Banking1*, *Banking2*, and *Banking3* (Dulá and López, 2012) have 4971, 12456, and 19939 points in 7, 8, and 11 dimensions, respectively. *MiniBooNE* (Dua and Graff, 2017) consists of  $n = 130,064$  data points in  $d = 50$  dimensions. The data set *RNA* (Uzilov et al., 2006) contains  $n = 488,565$  RNA input sequence pairs with  $d = 8$  features. A summary of all used data sets is provided in Table 1. Note that the appendix contains mainly data sets that are either small in terms of dimensions or number of data points. For that reason, they are arguably less relevant for archetypal analysis than the ones in the main body of the paper.

Figure 10 depicts the performance for the additional eight data sets. Note that we omit AA++MC 1% for small data sets, i.e., if  $n < 25,000$ . Again, we can see that Uniform and the FurthestSum initialization perform worse than the proposed approach and its approximation. AA++ is almost consistently best, except on some rare occasions, such as for  $k = 25$  on Concrete. While the MCMC approximations of AA++ performed very close to AA++ itself, we can see some more significant performance gaps on these additional data sets. Especially on BankProblem1, most Monte Carlo versions fail to approximate AA++ properly. For other data sets such as MiniBooNE and RNA, AA++MC using only 1% of the data as a chain length is a sub-optimal choice. However, note that all approximations are still better than the Uniform baseline.



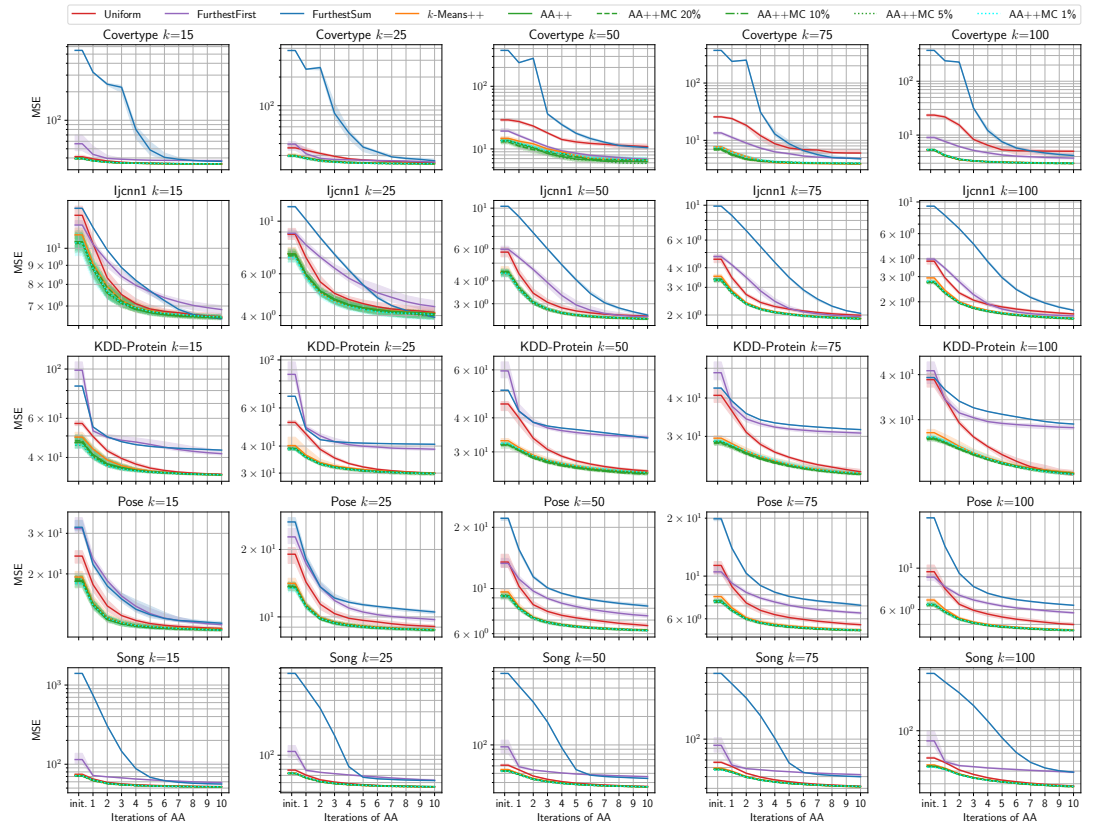
**Appendix C—Figure 10.** Results on Airfoil, California Housing, Concrete, Banking1, Banking2, Banking3, MiniBooNE, and RNA using the *CenterAndMaxScale* pre-processing as in the main body of the paper.

## D Results on Standardized Data Sets

We also conduct the same set of experiments on all data sets using standardization as pre-processing. In Figure 11, we can see for the first set of data sets that FurthestSum usually performs worst, often by a large margin. In contrast, the most consistent behavior has the proposed AA++ method, which is often the best. Besides, the proposed approximations of AA++ perform sufficiently close to AA++ itself.

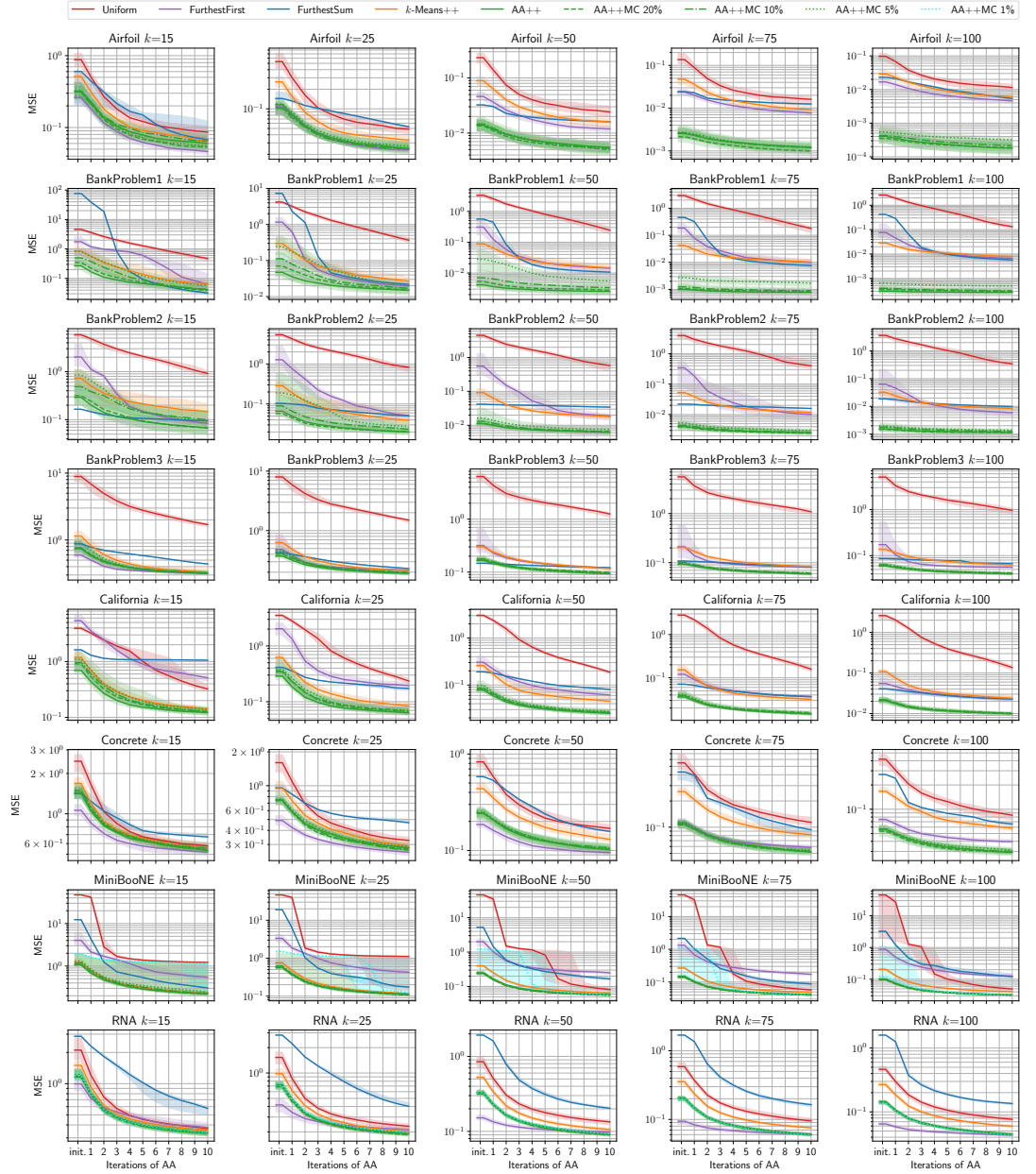
The performance on the second set of data sets is depicted in Figure 12. On those, Uniform is usually yielding the worst results. However, FurthestSum is also occasionally underperforming, especially on the RNA data set. Once again, the most consistent behavior is achieved by AA++, which is also often best. While the MCMC-based approximations are usually good,  $k$ -means++ still has a gap compared to AA++.

The results in Figures 11 and 12 are summarized in Figure 13. As expected, AA++ wins on most

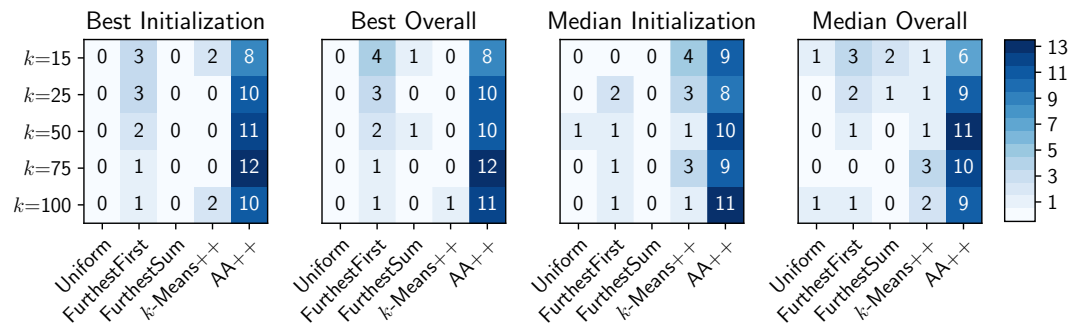


**Appendix D—Figure 11.** Results on Covertypes, Ijcnn1, KDD-Protein, Pose, and Song using standardization as pre-processing.

the data sets irrespective of the applied setting. However, the numbers are weaker than in Figure 7, which summarizes results using the CenterAndMaxScale pre-processing.



**Appendix D—Figure 12.** Results on Airfoil, California Housing, Concrete, Banking1, Banking2, Banking3, MiniBooNE, and RNA using standardization as pre-processing.



**Appendix D—Figure 13.** Aggregated statistics over 13 data sets (five data sets from above excluding MNIST and eight data sets from the appendix) using standardization as pre-processing. Each table shows how often each initialization method yields the best result for various settings of  $k$  under different settings. Best refers to the lowest single seed and median refers to the median over many seeds. We report on the performance after initialization and overall during the optimization.